DOPPLER MEASUREMENTS AS A SOURCE OF ATTITUDE INFORMATION FOR THE ULYSSES SPACECRAFT

J A Massart & A Schültz

European Space Operations Centre (ESOC)
Robert-Bosch-Str. 5, 6100 Darmstadt, FRG

ABSTRACT

Ulysses is a spinning spacecraft on an interplanetary trajectory whose prime objective is the exploration of the solar environment at high solar latitudes. When the spacecraft's spin axis is not pointed to the earth, the capability of the Attitude Measurement System is limited to the determination of the spin period and the sun aspect angle. This limitation of the Attitude Measurement System is highly critical for the first few days after the injection and for the first Trajectory Correction Manoeuvre (TCM). We demonstrate that the Doppler radiometric measurements, collected primarily to estimate the spacecraft trajectory, are a valuable source of attitude information and that the Attitude and Orbit Control System can be fully calibrated in flight using Doppler and sun data. We show that these special techniques can be used to determine the spacecraft attitude after injection and to ensure that the first Trajectory Correction Manoeuvre is accurately carried out.
Keywords: Attitude Determination, Thruster Calibration, Dopoler Signature, Tracking Data.

ABBREVIATIONS

AMS	Attitude Measurement System
AOCS	Attitude and Orbit Control System
CONSCAN	Conical Scanning
DSN	Deep Space Network
EAA	Earth Aspect Angle
ESA	European Space Agency
ESOC	European Space Operations Centre
FD	Flight Dynamics
HGA	High Gain Antenna
JPL	Jet Propulsion Laboratory
LGA	Low Gain Antenna
NASA	National Aeronautics and Space Administration
RCE	Reaction Control Equipment
RF	Radio Frequency
RTG	Radioisotope Thermoelectric Generator
SAA	Sun Aspect Angle
TCM	Trajectory Correction Manoeuvre

1. INTRODUCTION

1.1 Ulysses Mission

Ulysses is a joint ESA/NASA programme whose prime objective is the exploration of the solar system environment at high solar latitudes. To reach these latitudes, the spacecraft will be launched by the Shuttle in a low earth orbit and injected by an Upper Stage into an interplanetary trajectory aimed at Jupiter. The target point is selected in such a way that Jupiter's gravitational field will deflect the spacecraft into a solar polar orbit which brings it successively over the two poles of the sun.

The spacecraft, which carries a mixed US/European payload, is provided by ESA. NASA will launch the spacecraft and provide telemetry acquisition, tracking support and command transmission through its Deep Space Network (DSN). Spacecraft operations and control will be conducted by an operations team transferred from the European Space Operations Centre (ESOC) in Darmstadt, Germany, to the Jet Propulsion Laboratory (JPL) in Pasadena, California. The JPL team will determine the spacecraft trajectory and supply the scientific community with payload data. ESOC provides the software necessary to control the spacecraft, to verify the good performance of the payload and to design, execute and monitor attitude and Trajectory Correction Manoeuvres (TCM).

Spacecraft telemetry data and radiometric data (Doppler and Range) will be acquired by the DSN stations. In general there will be one eight hours contact period per day. During this period the station generates for the spacecraft an uplink carrier (S-Band) modulated by commands and ranging while at the same time it separates the spacecraft downlink signal (X or S-Band) in its components: Doppler shift, Telemetry and Ranging.

The telemetry transmitted by the spacecraft is routed to JPL where the real time telemetry is immediately processed in order to establish the health of the spacecraft and to verify the correct loading and execution of telecommands. The Flight Dynamics (FD) system evaluates the spacecraft attitude to derive the magnitude of the depointing of the High Gain Antenna (HGA) from the earth and to generate the commands necessary for an eventual correction. These will then be transmitted to the station and uplinked to the spacecraft. The small correction manoeuvres will normally be executed outside ground contact, so as not to disturb the communication link.

Proceedings of the Second International Symposium on Spacecraft Flight Dynamics, Darmstadt, FR Germany, 20–23 October 1986 (ESA SP-255, Dec. 1986)

Similarly the radiometric data recorded at the station are transmitted to JPL where they are routed to the Navigation System. While tracking the spacecraft, DSN generates so called Doppler 'pseudo residuals'. They represent the deviation between predicted and actual measurements and can be used to monitor, not only the spacecraft track, but also critical events such as attitude and orbit manoeuvres. The Navigation system evaluates the spacecraft trajectory and provides it to the FD system. There it is used together with telemetry and Doppler data, to compute and control the spacecraft's attitude and the critical TCMs necessary to correct the injection errors and to trim the trajectory before Jupiter swing-by. The Navigation system also provides DSN with predictions of the data necessary for the station to acquire and track the spacecraft.

1.2 The Spacecraft

1.2.1 Overview. The Ulysses spacecraft is shown in its operational configuration in Figure 1.1. It has a mass of 370 kg and is spinning at 5 rpm. The box type structure is dominated by the large parabolic HGA that provides the communication link with the earth and by the Radioisotope Thermoelectric Generator (RTG) that supplies the spacecraft electric power. In addition to the narrow beam HGA, two Low Gain Antennae (LGA) provide omnidirectional telemetry coverage during the first two weeks of the mission. Experiments requiring electromagnetic cleanliness and minimisation of the RTG radiation have been mounted on a 5.5 m radial boom located on the opposite side of the spacecraft to the RTG. This boom stowed during launch is released soon after injection. A 72 m tip to tip dipole wire boom and a 7.5 m axial boom, serving as electrical antennae, will be deployed one month later.

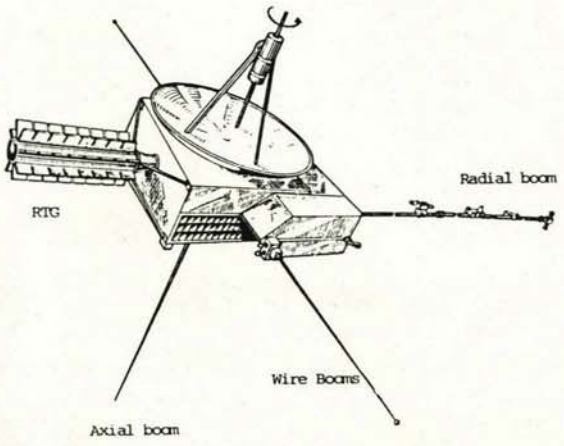

Figure 1.1. The Ulysses spacecraft

The HGA is aligned with the spacecraft spin axis which must periodically (ca. every day) be realigned with the Earth direction in order to maintain the communication link. The size and direction of the required attitude adjustment manoeuvres are derived onboard by a CONSCAN system which senses a radio frequency (RF) signal sent from the ground station to the spacecraft. To completely determine its attitude, the spacecraft is also equipped with two redundant sun sensors which provide spin rate, spin phase and sun aspect angle information.

The Reaction Control Equipment (RCE) which carries out, not only the small attitude trimming manoeuvres, but also the large TCMs, consists of a single fuel tank (with a capacity of 34 kg of hydrazine) and eight 2 N thrusters.

The Attitude and Orbit Control System (AOCS) is highly sophisticated and includes many autonomous control loops and failure detection functions to assure fail safe operations, particularly when the spacecraft is not visible from a ground station.

The Communication system provides capability for telemetry (with bit rates up to 8 kbits/s), ranging and telecommand. It operates in X-Band (downlink) and S-Band (up- and downlink). The S-Band antenna beam is slightly offset from the X-Band beam (itself aligned with the spacecraft spin axis) to enable RF sensing of the attitude pointing error with the CONSCAN system.

1.2.2 Measuring the spin period, spin phase and sun aspect angle. The spinning motion of the spacecraft causes the sun to cross the slits of one or more sun sensors. The transit times of the sun in the slits of an X-beam sensor provide the data necessary to estimate the spin period, the spin phase and the sun aspect angle. This X-beam sun sensor contains two slits having a field of view of 120 deg x 1 deg. One slit is parallel to the spacecraft meridian plane. The other is tilted at an angle of 14 deg. Both slits intersect 40 deg above the spacecraft equatorial plane. The meridian slit overlaps the spin axis by an angle of 10 deg; the sun crosses it twice per spin in the overlapping region.

When the sun crosses a slit, a pulse is generated by the detector and routed to the electronics where its leading and trailing edges are datated and stored in registers, each update overwriting the previously stored datation of the same type. These datations are sampled in the telemetry stream with a frequency which depends on the bit rate and on the type of telemetry format (short Engineering or long Science) that is being generated. Sampling frequencies may vary between 2 and 512 sec for a nominal spin period of 12 sec (or 6 sec during large TCMs). On reception at JPL, the sequence of sun transit times is extracted from the telemetry and processed to provide instantaneous values of the spin period and the sun aspect angle. An initial guess is used to solve ambiguities caused by low sampling rates, if two successive datations are separated by many spin periods. This initial estimate is normally provided by a smoothing process carried out on the instantaneous values. Alternatively an estimate computed onboard can be used. The smoothing process carried out on ground is based on a Kalman type filter whose statistical properties (system noise, measurement noise, initial uncertainties) are dictated by the actual spacecraft dynamic configuration (pure spin or actively controlled, with or without deployment of the flexible appendages, etc.).

The spin period is determined first and its estimate is used to compute the sun aspect angle, for which two different methods are used. Figure 1.2 illustrates the two measuring principles. For large sun aspect angles (e.g. larger than 12 deg) the sun crosses both the meridian and oblique slit of the X-beam sensor. The difference in crossing times of the two slits is then a measure of the sun elevation. Unfortunately, in the telemetry stream, both crossings may differ by many spin periods and, for the oblique pulse, only the trailing edge is available. Particular care is therefore exercised when processing this type of information to derive a sun aspect angle. In practice, a spin angle (which corresponds to the time interval separating the trailing edge of the meridian slit from the trailing edge of the oblique slit) is constructed and a look up table is interpolated to derive the corresponding sun aspect angle. This look up table takes into account the spin axis tilt and will be updated when new estimates become available. For small sun aspect angles the sun cannot cross the oblique slit. Then the time difference between the leading edge and the trailing edge of the meridian slit pulse becomes the prime measure of the sun aspect angle. Here also, special care is taken to cope with spin axis tilt and datations that do not belong to the same spin period.

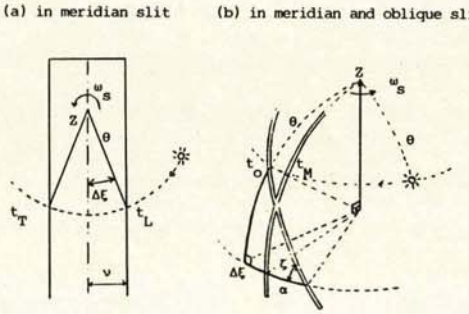

Figure 1.2. Sun aspect angle calculation

The spin axis tilts are essential parameters to the above process and are easily obtained inflight when the sun is in the meridian slit's overlapping region and crosses the slit twice per spin period. Figure 1.3 illustrates the basic principle. An offset of the spin axis from the sensor optical plane yields a discrepancy between the time difference separating the leading edge of the first pulse from the trailing edge of the second pulse, and the time difference separating the trailing edge of the first pulse from the leading edge of the second pulse. This provides the component of the spin axis tilt orthogonal to this slit. Since the spacecraft is equipped with a second X-beam sensor whose meridian slit is orthogonal to the one of the first sensor, the second orthogonal component is also available.

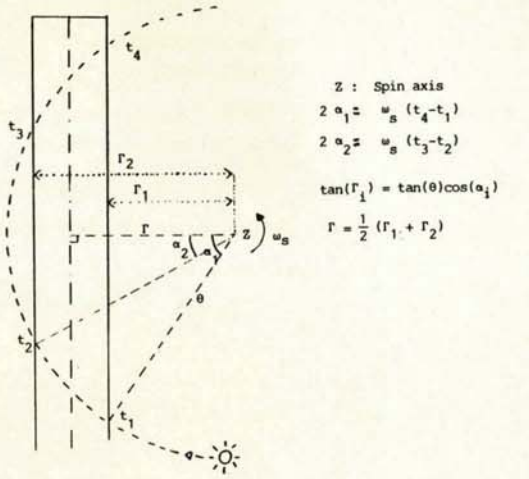

Figure 1.3. Estimation of the spin axis tilt

1.2.3 Measuring the earth aspect angle and phase. The HGA S-Band boresight is slightly offset (1.8 deg) from the spin axis. Hence the antenna gain pattern is not symmetric with respect to the spin axis. This causes a slight decrease in the signal level at the receiver's input if the direction of the incoming signal (i.e. the ground station) is aligned with the spin axis. If, however, the spin axis is depointed from the earth, a modulation of the strength of the incoming signal takes place at the spin frequency. The amplitude of the modulation is proportional to the size of the offset of the spin axis from the earth. Its phase is related to the phase of the earth with respect to the spacecraft meridian plane containing the tilted S-Band feed. This is illustrated in Figure 1.4.

The Receiver's AGC signal, containing this modulation, is transmitted to a 'CONSCAN' processor to derive its amplitude and phase with respect to the sun. This processor is also provided with the spin frequency, derived from the sun pulses, in the form of two square waves approximating cos (ωt) and sin(ωt) and phased with respect to a sun reference pulse. By convoluting the input signal with these basic square waves for two complete spin periods, the processor generates two signals $X = A \sin(\varphi)$ and $Y = \cos(\varphi)$ from which the amplitude A and phase φ are readily obtained.

Onboard the processor handles earth offset angles of 5 to 6 deg. The amplitude and phase derived by the measuring electronics are provided to the Conscan control electronics which, if enabled, precesses autonomously the spin axis towards the earth within a dead band of ca. 0.1 deg. The measuring electronics store the X and Y output of the integrators in two 8-bits registers which are regularly sampled in the telemetry. Earth aspect

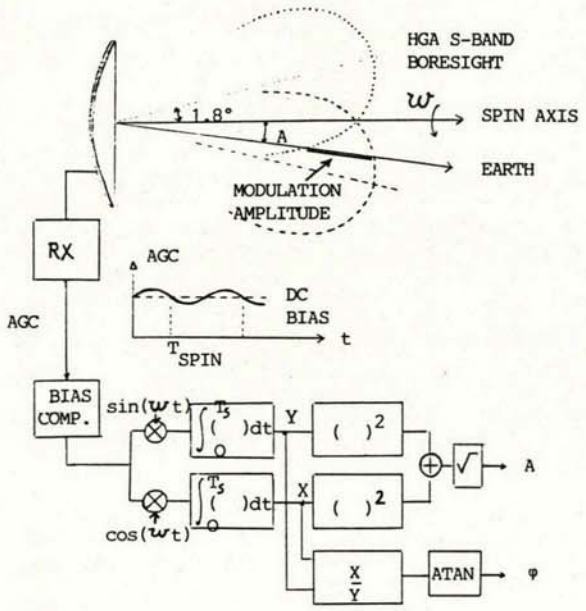

Figure 1.4. The CONSCAN principle

angle and phase can then be calculated on ground and merged with sun aspect angles to reconstitute the complete attitude. The maximum amplitude of the X and Y signals included in the telemetry has been limited to 2.25 deg since an optimal downlink can only be achieved for small depointing angles (less than 0.5 deg).

1.2.4 Executing attitude and orbit control manoeuvres. Figure 1.5 illustrates the location of the thrusters on the spacecraft platform. All thrusters can be fired either in a continuous mode or a pulsed mode. To satisfy a diversity of mission requirements, the pulsed mode supports a large range of duty cycles.

Attitude precession manoeuvres use one or two axial thrusters firing once per spin or every second spin. The balanced mode uses one upper and one loweraxial thruster to reduce as much as possible the resulting velocity changes which affect the spacecraft trajectory. Spin rate correction manoeuvres use one or more spin thrusters in pulsed mode.

Trajectory Correction Manoeuvres can be carried out in two different ways. In the first mode, the spin axis is precessed to the direction parallel to the required velocity increment, two axial thrusters are fired to provide a delta-v parallel to the spin axis direction, and the spin axis is then returned to its earth pointing direction. This mode will only be used when a telemetry downlink can be maintained through the LGA. In the second mode the spacecraft stays pointed at the earth and the velocity increment is decomposed in a component parallel to the spin axis and a component perpendicular to the spin axis. Fuel efficiency dictates that the delta-v perpendicular manoeuvre is carried out first.

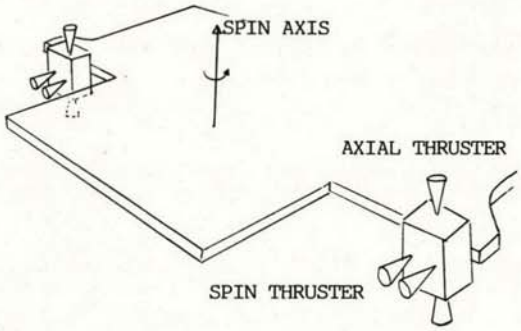

Figure 1.5. Thruster location

1.2.5. Preparing attitude and orbit manoeuvres. When computing the manoeuvre commands, the software takes into account the individual performances of each thruster. These performances are derived from the 'thruster acceptance tests' which provide records of the thrust level, the thrust centroid and the specific impulse against number of pulses for different propellant supply pressures. A typical transient behaviour of the thrust level and the specific impulse is illustrated in figure 1.6. One sees that for a given injection pressure they can be modelled as exponential functions of the form

$$F(p) = F_\infty \left(1 - A_e^{-K(p-1)}\right)$$

where F(p) is the thrust level for pulse p
F_∞ is the steady state thrust level
A and K are the parameters obtained through a least squares fit.

When modelling the spacecraft performance the software computes for every spin period and for each thruster activation the resulting force and torque in body axes, and the fuel used. Then, in inertial coordinates, it computes the velocity increment and the change in angular momentum. After each spin period the new fuel mass is used to adjust the injection pressure and hence the thrust level for the following pulses.

When calculating manoeuvre parameters the program iterates. For example, for a precession manoeuvre the program starts by computing the rhumb line parameters (angle and length) and convert them in spacecraft parameters such as a number of pulses and a thrust pulse phase delay with respect to the spin axis-sun plane (assuming a constant precession rate computed from input parameters representing the spacecraft status at the start of the manoeuvre). Then the manoeuvre is simulated step by step, each step corresponding to one spin period. The resulting end attitude is compared to the desired one and the initial conditions (number of pulses, thrust phase delay) are automatically adjusted to start a new iteration. The iterations terminate when the differences between desired and achieved attitudes are such that they fall below the resolution of the telecommands. The program provides, at the start of every spin period, intermediate values of essential monitoring parameters such as the sun aspect angle, the earth

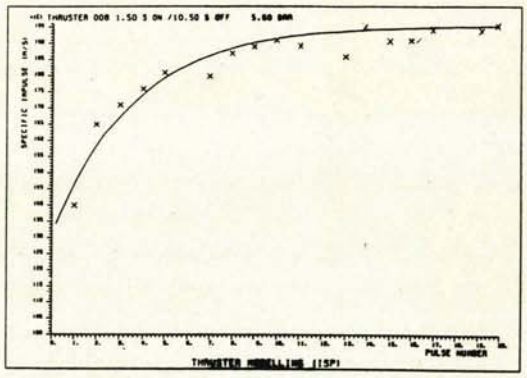

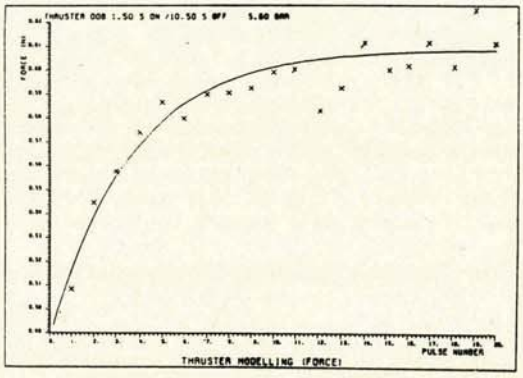

Figure 1.6. Transient thrust level as function of pulse number

aspect angle, the spin rate, the radial component of the velocity increment, etc.

1.3 Critical Flight Operations

After injection and acquisition of the spacecraft by a DSN station, the flight control team will check the nominal performance of the spacecraft whose transmitter will be connected to the LGA. In particular the spacecraft spin period and sun aspect angle will be verified. Since at that time the spacecraft is not pointed at the earth, the full attitude cannot be reconstituted. Next, the radial boom will be deployed and the spin rate adjusted to its nominal value of 5 rpm.

Then the attitude reorientation manoeuvres necessary to acquire the earth with the HGA will start. These manoeuvres will be performed in a way that allows in-flight calibrations of the thrusters and verification of the alignment of the HGA with the spin axis. In order not to interfere with the determination of the spacecraft trajectory and the assessment of the injection errors, the earth acquisition exercise is split in two parts separated by four days during which the trajectory will not be perturbed by activation of the thrusters. During this time interval the spin axis will be directed within a few degrees of the sun in order to evaluate the spin axis tilts. The earth acquisition will be completed 8 to 10 days after injection.

The FD team will now generate the sequence of manoeuvres necessary to reach the target at Jupiter. The first TCM will be carried out 10 to 12 days after injection. Using more than fifty percent of the fuel, its success is vital to the mission. Real time processing of the spacecraft telemetry (to assess the spacecraft's performance) and of the stations's doppler residuals (to monitor the change in radial velocity) will therefore be carried out.

During the next two weeks, the trajectory is re-evaluted and the thrusters can be calibrated by comparing the manoeuvre actually carried out with the predictions. These calibrations together with the newly estimated orbit are then used to calculate the second TCM which will be executed four weeks after injection. Later the 72 m tip-to-tip wire booms are deployed and the spin rate adjusted. This critical manoeuvre will be closely monitored in order to ensure a symmetrical deployment of both wires. Next the axial boom is deployed and this terminates the critical early orbit phase.

The spacecraft now enters in its routine operations phase characterised by the periodic attitude precession manoeuvres necessary to keep the HGA pointed towards the earth.

On its way to Jupiter the spacecraft will still meet two critical periods: the first opposition and the first conjunction. During these periods, the sun and the earth will appear in line when seen from the spacecraft. Special attitude manoeuvering strategies will be used in order to satisfy the radio science requirements without endangering the spacecraft by pointing the spin axis to the sun. During conjunction, the sun will lie between the spacecraft and the earth and block out communications for a few days.

Two weeks prior to Jupiter's encounter, the Ulysses trajectory relative to Jupiter will have been established and a third TCM can take place to trim the arrival parameters to the target parameters. The target is selected so that the spacecraft is deflected out of the ecliptic plane on a heliocentric orbit passing successively over the two poles of the sun. Trajectory Correction Manoeuvres are no longer relevant after fly-by, and only daily precession manoeuvres will be necessary to keep the HGA pointed at the earth. Two further oppositions and conjunctions take place after Jupiter encounter. The scientific mission is terminated after the crossing of Ulysses over the second pole of the sun, when the spacecraft's heliographic latitude drops below 70 deg.

2. USE OF DOPPLER DATA IN THE FLIGHT DYNAMICS SYSTEM

2.1 Basic Principles for Doppler Measurements

2.1.1 Measuring 'two-way Doppler' at the ground station. Neglecting relativistic effects, the Doppler shift between the frequency f_T transmitted by a source and the frequency f_R measured by a receiver moving with radial velocity $\dot{r}$ with with respect to the transmitter is obtained from the relation

$$f_R = f_T (1 - \dot{r}/c)$$

where c is the speed of light.

The principle used to measure the spacecraft's Doppler shift at the ground station is illustrated in Figure 2.1 for the 'two-way Doppler' system.

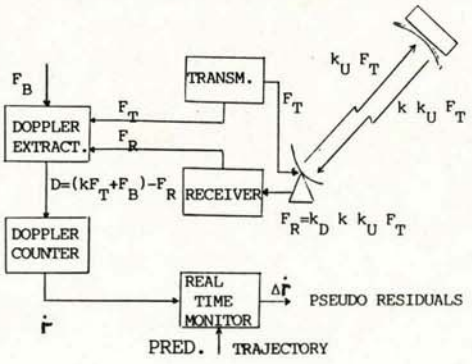

Figure 2.1. Generation of Doppler residuals for two-way Doppler tracking

At the station the transmitter generates the uplink carrier of frequency f_T. The spacecraft radial velocity $\dot{r}$ relative to the station causes it to detect a signal whose frequency equals the transmitted frequency multiplied by the Doppler uplink factor $k_U (= 1 - \dot{r}_U/c)$. The spacecraft translates this frequency $k_U f_T$ in its downlink frequency by multiplying it by the 'turn around ratio' k (= 240/221 in S-Band) of the transponder. The resulting signal of frequency $k\ k_U\ f_T$ is generated by the spacecraft as downlink carrier. This signal, affected by the downlink Doppler factor k_D (=1 - $\dot{r}_D/c$), is detected by the stations's receiver as a signal of frequency $f_T = k_D\ k\ k_U\ f_T$. It is then passed to the Doppler extractor where the incoming frequency f_R is compared to the transmitted frequency f_T multiplied by the spacecraft's transponder turn around ratio k. The Doppler Extractor gives an output signal whose frequency D is represented by

$$D = (k \cdot f_T + f_B) - f_R$$

where f_B is a bias frequency (typically 1 MHz), added to $k\ f_T$, to ensure that the resulting frequency is always larger than f_R (so that we can later distinguish between negative and positive Doppler shifts).

The output of the Doppler Extractor is fed to a Doppler Counter which increments by one at the beginning of each cycle of its period input signal D and, at the instant of sampling, resolves the phase (fractional cycle) of the cycle in progress. This counter has a resolution of 0.001 Hz and is regularly sampled (e.g. every 0.1 sec) to save the data. A Doppler frequeny may then be retrieved from this record in the form of an average frequency between sample times.
In the above description, the spacecraft's transponder generates the downlink frequency by reference to the uplink. This produces 'two-way coherent Doppler' if it is being measured by the same station that is providing the uplink signal; otherwise the station that is receiving, but not transmitting, measures 'three-way Doppler'. If the spacecraft uses its internal frequency reference to generate the downlink, the Doppler produced by the Doppler Extractor are called 'one-way Doppler'. Note that the incoming frequency f_R is treated in exactly the same way regardless of its origin.

2.1.2 Generation of Doppler pseudo residuals. While monitoring the performance of the tracking system, the 'real time monitor' program compares the measured Doppler frequency to predictions based on the best available spacecraft trajectory and on the known motion of the station. To produce Doppler residuals the computer calculates a Doppler frequency from the original samplings of the Doppler Counter. To reduce the noise level in the Doppler frequency, one selects samples separated by a larger time interval, typically in the range 1 to 60 sec depending primarily on expected spacecraft activities. The resulting average frequency is then compared to the predicted and pseudo residuals, expressed in milliHz, are generated (these residuals are called 'pseudo' in order to dissociate them from the residuals obtained during the orbit determination process). Inadequate performance of the tracking system will be reflected in the Doppler residuals, either as large biases (e.g. incorrect frequency settings...) or excessive noise (e.g. instabilities in the receiver phase lock loop, errors in the timing system...). Normally the residuals will be small: inaccuracies in the trajectory contribute only to a fraction of a Hertz in cruise phase, although this may be strongly magnified near a gravitating body. Since spacecraft manoeuvres are not modelled in the predictions, they will be directly apparent if they affect the spacecraft radial velocity. Residuals will suddenly start to ramp when a manoeuvre is activated. Figure 2.2 illustrates the occurence of four small attitude precession manoeuvres of the Pioneer Venus orbiter. At that time the spacecraft to sun separation as seen from the earth was small, explaining the high level of noise apparent on the illustration.

2.1.3 Conversion to radial velocity measurements For a two-way Doppler system, the Doppler frequency D can be related to the spacecraft radial velocity by observing that, for sufficiently slowly varying radial velocity, $\dot{r} = 0.5\ (\dot{r}_U + \dot{r}_D)$ and $f_R = k\ f_T\ (1 - 2\dot{r}/c)$. This yields

$$\dot{r} = (D - f_B) \cdot c/(2k\ f_T)$$

The Ulysses spacecraft has an S-Band downlink frequency $k\ f_T$ centered at 2293.14815 MHz; this gives a ratio of 15.29 Hz per m/sec. In general Doppler frequencies expressed in Hz are converted to radial velocities expressed in m/sec by multiplying them by the factor

$$F = c/(k\ f_T\ n)$$

where n = 1 for one-way Doppler and n = 2 for two- and three-way Doppler.

2.1.4 Accuracy of radial velocity. When converted to m/sec, the residual Doppler frequencies provide us with the difference between the predicted spacecraft radial velocity and the one measured through the Doppler shift. Under normal conditions, the noise in the Doppler frequencies is ca 0.1 Hz for a 1 sec sampling period. As the

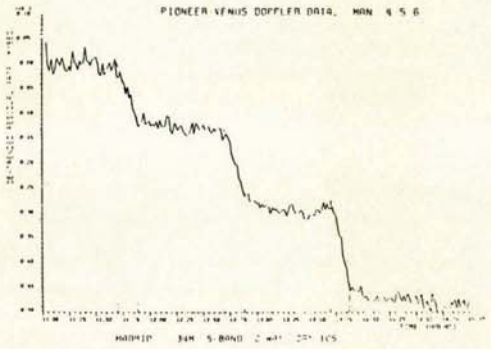

Figure 2.2. Precession manoeuvres of Pioneer-Venus orbiter

noise reduces with $1/\sqrt{s}$, an accuracy of 1 mm/s will be achieved for a sampling period of 60 sec. This provides visibility of many small changes in the radial velocity of the spacecraft's radiating source.

Although the average residual velocity should ideally be zero, this is generally not the case: slowly moving biases originating from inaccurate predictions are usually present. We show in section 2.3 that they can easily be taken care of.

2.2 Visibility of Attitude Motions on Doppler Data

2.2.1 The effect of spacecraft spin. For two-way Doppler data, the spinning circularly polarised antenna of Ulysses drops 1 cycle for each revolution when it receives the signal sent from the station and drops k (= 240/221) cycles when it transponds the signal. This loss results in a frequency bias of $(1 + k)\ f_z$, where f_z is the spacecraft spinning frequency. For the 5 rpm spin rate of Ulysses it amounts to 0.1738 Hz (or 1.1 cm/sec). This bias is taken into account by the Navigation system when estimating the spacecraft trajectory.

Ulysses rear LGA is mounted at a distance h (ca. 1.2 m) of the spacecraft's spin axis. Therefore the radio centre of the antenna has a circumferential velocity v_c (=$h\omega$) relative to the spacecraft's centre of mass. The radial component (i.e. the projection on the earth direction) of the rotating velocity vector oscillates in a simple harmonic motion (see Figure 2.3) and is described by

$$v_R(t) = v_C \sin(\omega t)\ \ \sin(EAA)$$

This oscillation at the spin frequency is superimposed on the radial velocity of the centre of mass and is reflected in the Doppler data. Now, when computing residuals from the sampled Doppler counts, the station's Real Time Monitor program removes the effect of the predicted radial velocity of the centre of mass thereby leaving, in the residual frequencies, the effect of the antenna motion with respect to the centre of mass. This sine wave in the Doppler residuals is normally sampled at discrete time intervals

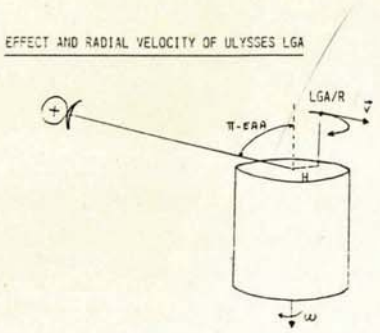

Figure 2.3. Rear antenna geometry

(e.g 1 data every sec, 1 every 10 sec or 1 every 60 sec, etc.), and each sampled point corresponds to an average frequency over the sample time interval. For a sampling period of s sec, the average at time tn is given by

$$\frac{1}{s}\int_{t_n - s}^{t_n} v(t)dt$$

This yields

$$v_R(t_n) = \left(\frac{2}{s}\right) h \sin(EAA) \sin\left(\omega \frac{s}{2}\right) \sin\left(\omega\ (t_n - \frac{s}{2})\right)$$

which can be written in the form

$$v(t) = v_C \cdot \mu(s) \cdot \sin(EAA) \cdot \sin(\omega\ t - \varphi)$$

where

$$\mu(s) = \frac{\sin(\omega \frac{s}{2})}{\omega \frac{s}{2}} \qquad \text{and } v_C = h\omega$$

The amplitude

$$V = v_C \cdot \mu(s)\ \ \sin(EAA) \qquad (1)$$

depends on the velocity v_C of the antenna radio centre, the earth aspect angle EAA and the attenuation factor $\mu(s)$ which represents the averaging effect caused by the discrete sampling. As can be seen from Figure 2.4, this attenuation factor is close to 1 from small averaging times and tend to 0 for very large sampling periods.

For Ulysses (5 rpm, h = 1.2 m), a 1 sec sampling period yields an amplitude in the oscillations of the radial velocity of 621 mm/s for a 90 deg EAA, reducing to 10.3 mms for a 1 deg EAA.

If the sample period is close to a multiple of the spin period a beat effect will take place (see Figure 2.5).

The zero crossings of the sine wave take place when the circumferential velocity of the antenna is orthogonal to the plane containing the spin axis and the earth. Therefore by relating the Earth Received Time of the signal to the Spacecraft time, the phase of the oscillation in the Doppler residuals gives the position of the rotating antenna with respect to that plane.

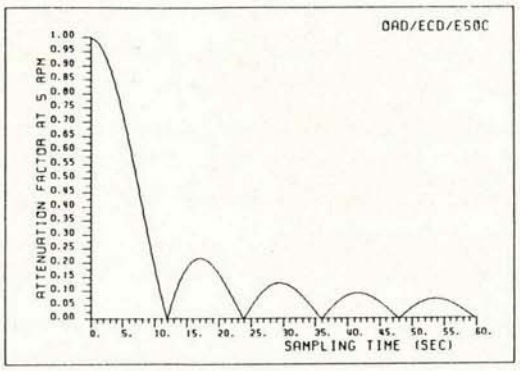

Figure 2.4. Attenuation of amplitude as function of sampling period

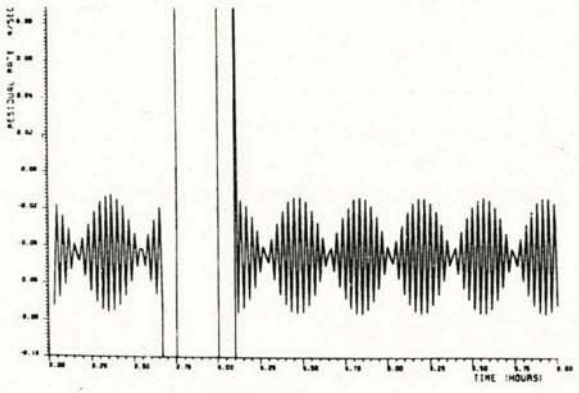

Figure 2.5. Multiprobe orbiter Doppler residuals

The time of the zero crossing can then be combined with the time at which the sun crosses the meridian slit of the XBS sensor to derive the phase angle between the plane (spin axis - sun) and the plane (spin axis - earth). When computing the attitude from intersections between the sun cone and the earth cone, this angle is used to select one of the two possible intersections.

2.2.2 The effect of attitude/orbit manoeuvres. The effect of manoeuvres on the spacecraft velocity is detected in the Doppler residuals. Precession manoeuvres carried out in the unbalanced mode (i.e. using one axial thruster) induce a velocity change of the centre of mass in a direction parallel to the spin axis. The radial component of this delta-v is observed in the Doppler residuals. During the manoeuvre, the spin axis moves around the sun on a rhumb line trajectory, changing gradually the direction of the velocity increment and the size of its projection on the earth line. The total change in the residual velocity represents the component along the earth line of the cumulated velocity increments imparted during the manoeuvre. If the precession manoeuvres are carried out in a balanced mode (i.e. using two axial thrusters giving opposite velocity increments) the net resulting force should ideally be zero. In this case the change in radial velocity will reflect effects such as thruster mismatch and plume impingement.

During the routine phase of the mission, daily precession manoeuvres of ca. 0.5 deg will keep the HGA pointed to the earth. The resulting velocity increment ($\simeq$6.4 mm/s) is along the earth line and directly observable in the Doppler residuals. Such manoeuvres are normally carried out in unbalanced mode since their cumulative effect is used to bias the Jupiter arrival conditions by selecting the axial thruster (upper or lower) which will yield the desired effect.

Spin rate correction manoeuvres are also detected on the Doppler residuals. Changes in the spin rate affect the bias shift caused by the circular polarisation of the antenna signal. Furthermore, if the spacecraft's rear LGA is used, the frequency of the oscillation will adjust to the new spin frequency. Spin rate corrections which are carried out in pulsed mode by firing one spin thruster once per spin period will induce a velocity change (nominally 8.0 mm/s per pulse) of which the radial component will be visible in the Doppler residuals. This component can be maximised by properly selecting the phase of the thruster firing. If the manoeuvre is executed by firing the spin thruster twice per spin period, half a period apart, the net velocity change per spin period should average to zero, but individual firings will be apparent for fast sampling rates of the Doppler counts.

The radial component of velocity changes imparted during trajectory control is observable in the Doppler measurements. For the nominal spin period of 12 sec, the 4 spin thrusters used together impart a delta-v of 33 mm/s (for a 45 deg pulse width) in a direction orthogonal to the spin axis; the 2 axial thrusters used in continuous mode yield 131 mm/s each spin period in a direction parallel to the spin axis.

2.3 Use of Doppler Data for Flight Dynamics

2.3.1 Measuring the earth aspect angle. When the rear LGA is used, the spin signature in the Doppler can be used to compute the EAA from (1). The amplitude V and phase φ of the oscillations in the radial velocities can be estimated by fitting a sine wave at the spin frequency through the residual radial velocities. Long term trends and any residual bias are taken care of in the estimation process. The accuracy σ_V of the estimated amplitude depends of the noise in the residual Doppler frequencies and of the number of measurements. By taking 10 to 15 minutes of data, the amplitude can be estimated to an accuracy better than 1 mm/s.

The accuracy of the EAA derived from (1) can be analysed as function of the three sources of inaccuracies: σ_V = 1 mm/s, σ_h = 5 mm and σ_ω = 5.10^{-5} rad/s. We have:

$$\sigma^2_{EAA} = \left|\frac{s}{2h\sin\frac{\omega s}{2}\cos(EAA)}\right|^2 \sigma_V^2 + \left|\frac{\tan(EAA)}{h}\right|^2 \sigma_h^2 + \left|\frac{s\tan(EAA)}{2\tan(\omega\frac{s}{2})}\right|^2 \sigma_\omega^2$$

This shows two singularities: first when $\omega \cdot s/2$ is

a multiple of π (i.e. when the sampling period is a multiple of the spin period) and second, when the EAA approaches $\pi/2$. The contribution of the different sources of error is illustrated in figure 2.6 for different sampling periods. We see that a large sampling period will provide inaccurate estimates of the EAA and that, for lower sampling periods, the dominant contribution to the uncertainty comes from the 5 mm uncertainty in the distance of the antenna from the spin axis. The high accuracy of the spin period makes negligeable its contribution to σ_{EAA} as long as the sampling period is not a multiple of the spin period. Figure 2.7 shows the rss of the three contributions for a range of sampling intervals. We see that an accuracy of 1 deg in the EAA can only be achieved for EAA below 75 deg and sampling periods which do not attenuate to much the signal.

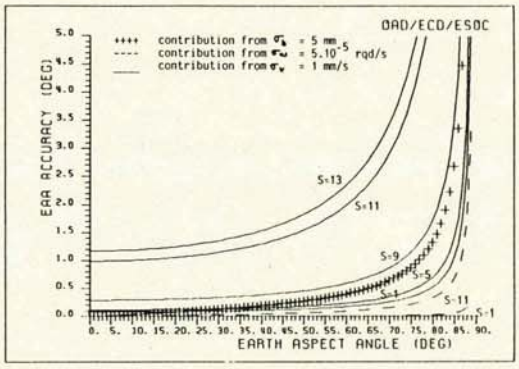

Figure 2.6. Earth Aspect Angle Accuracy for the 3 Error Sources

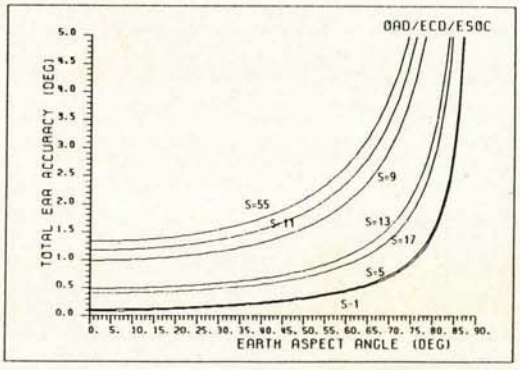

Figure 2.7. Earth Aspect Angle Accuracy for Different Values of s

2.3.2 Calibrating the thrusters efficiency

Without resorting to orbit determination, which may take a few days and attitude determination, which is limited to sun aspect angle and spin period, we shall highlight the conditions under which the Doppler residuals acquired during axial and radial delta-v manoeuvres contain sufficient information to calibrate the thrust force and the thrust centroid. Throughout this section we shall work with the following assumptions:

- the radial component $\Delta\dot{r}$ of the velocity change Δv can be estimated to an accuracy $\sigma_{\Delta\dot{r}}$ = 1 mm/s
- continuous axial delta v manoeuvres will have a minimum length compatible with the 32 sec resolution of the onboard time tag, Δv = 350 mm/s
- pulsed radial manoeuvres have a minimum of 25 thruster actiations; this provides a minimum Δv = 660 mm/s

We shall aim at calibratim the thrust efficiency to 1% and the thrust centroid delay to a angle of 1 deg (for a 45 deg pulse width).

Axial delta-v calibration of thrust efficiency

Denoting by k the thrust efficiency factor, by $\Delta\dot{r}$ the radial component of the velocity increment Δv estimated from the Doppler residuals, and by η the angle between the delta-v direction and the earth direction (i.e. the EAA for axial manoeuvres), we have

$$k\,\Delta v\cos\eta = \Delta\dot{r} \qquad (2)$$

where Δv is the velocity increment predicted by the manoeuvre preparation software.

The accuracy σ_k of the estimate derived from (2) is a function of the measurement accuracy $\sigma_{\Delta\dot{r}}$ and the model error σ_η (i.e. σ_{EAA}). We have

$$\sigma_k^2 = k^2\left(\frac{1}{\Delta\dot{r}^2}\,\sigma_{\Delta\dot{r}}^2 + (\tan\eta)^2\sigma_\eta^2\right) \qquad (3)$$

Figure 2.8 shows the different contributions to σ_k, as function of η, for different uncertainties σ_η (i.e. the attitude error). We see that the measurement uncertainty $\sigma_{\Delta\dot{r}}$ is negligeable as long as η stays below 70 deg. and that large attitude uncertainties will yield inaccurate estimates when η increases above a few degrees. This contribution of σ_η to σ_k is illustrated in figure 2.9 where we show, as function of σ_η, the maximum η for which σ_k will still be below 1%.

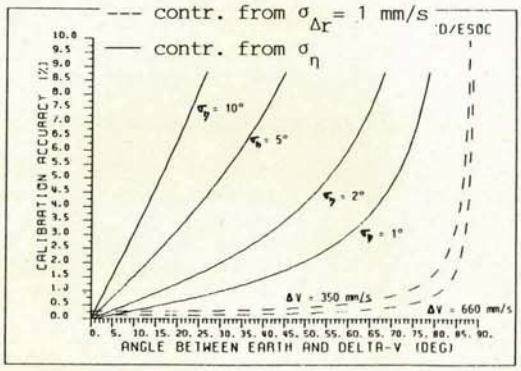

Figure 2.8. Thrust Efficiency Calibration for Delta-V

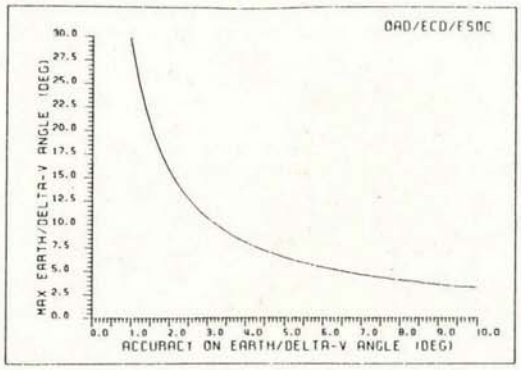

Figure 2.9. Constraint between Uncertainty and Maximum Δ V Offset Angle to Reach 1% Calibration Accuracy

Consequently, the calibration of the axial delta-v manoeuvre should be carried out in the "Earth pointing attitude", when $\eta = 0$ and $\Delta\eta$ is small.

Radial delta-v calibration

Radial delta-v manoeuvres use the spin thrusters in a pulsed mode with 45 or 90 deg pulse width. These manoeuvres will be calibrated, when the spin axis is orthogonal to the earth direction, by producing two velocity increments of equal size in two orthogonal directions around the spin axis. The first Δv increment will be such that the nominal thrust centroid is aligned with the Earth, whereas the second Δv increment will take place 90° after the first one. The Doppler residuals will provide the radial component $\Delta\dot{r}_1$ and $\Delta\dot{r}_2$ of both velocity increments. Figure 2.10 illustrates this basic principle used to derive the thrust efficiency factor k and the thrust centroid δ_c from $\Delta\dot{r}_1$, $\Delta\dot{r}_2$ and Δv. There it is assumed that the spin axis (Z) is exactly orthogonal to the Earth (E) and that the phase angle ξ (between the plane (Z, S) and the plane (Z,E)) at which the thrust centroid must occur, is perfectly known. In practice these assumptions do not hold: although we know accurately the sun aspect angle, we cannot determine accurately the phase around the sun or the earth aspect angle. The effect of an incorrectly assumed attitude is illustrated in figure 2.11. The phase error $\Delta\alpha$ (in the spin axis position around the sun) causes an error $\Delta\xi$ in the phase of the thrust centroid with respect to the real (Z_R,S) plane, and an error ΔEAA in the earth aspect angle. If the SAA is small a small error Δz will yield a large error $\Delta\alpha$ which in turn yields an error $\Delta\xi$ (nearly equal to $\Delta\alpha$).

Figure 2.12 illustrates this effect. There one has plotted $\Delta\xi$ as a function of the sun aspect angle for different values of Δz. This magnification of error between Δz and $\Delta\xi$ does not occur between Δz and ΔEAA, for which the

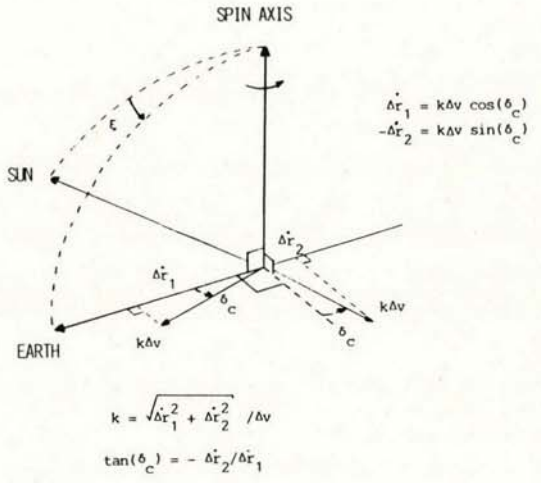

Figure 2.10. Calibration of radial delta-v

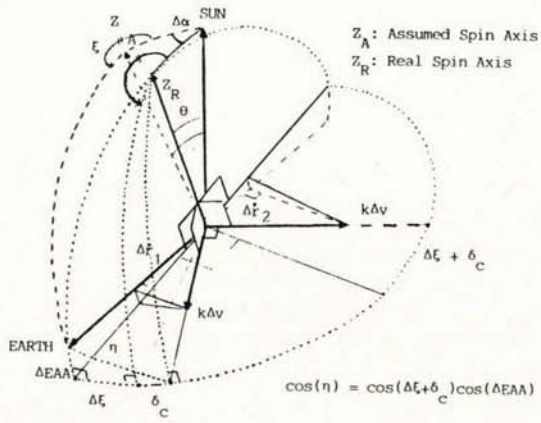

Figure 2.11. Effect of attitude uncertainty on radial delta-v calibration accuracy

maximum magnification fator is 1. The radial component of the 2 velocity increments is given by:

$$\Delta\dot{r}_1 = k\,\Delta v \cos(\Delta\xi+\delta_c)\cos(\Delta EAA)$$

$$-\Delta\dot{r}_2 = k\,\Delta v \sin(\Delta\xi+\delta_c)\cos(\Delta EAA)$$

from which we derive the thrust efficiency factor

$$k = \sqrt{\Delta \dot{r}_1^2 + \Delta \dot{r}_2^2} \; / \; (\Delta v \cos (\Delta EAA)) \qquad (4)$$

and the thrust centroid delay calibration δ_c from

$$\tan(\Delta\xi + \delta_c) = \frac{-\Delta r_2}{\Delta r_1} \qquad (5)$$

In practice we do not know ΔEAA and $\Delta\xi$. Therefore by assuming them to be zero our estimates $\hat{k}$ and $\hat{\delta}_c$ will be in error. It is readily observed that if ΔEAA (or Δz) is limited to 6° then the differences between $\hat{k}$ and k is less than 0.5%. We can show that σ_k computed from (4) is identical to (3) if η is replaced by ΔEAA and $\Delta \dot{r}^2$ by $(\Delta \dot{r}_1^2 + \Delta \dot{r}_2^2)$. Therefore the same conclusions apply as for axial delta-v manoeuvres: the attitude must be known to better than 5° for a reliable estimate of k.

From (5) we can show that

$$\sigma^2_{\Delta\xi + \delta_c} = \frac{1}{(\Delta \dot{r}_1^2 + \Delta \dot{r}_2^2)} \; \sigma^2_{\Delta \dot{r}} \approx \frac{\sigma^2 \Delta \dot{r}}{\Delta v^2}$$

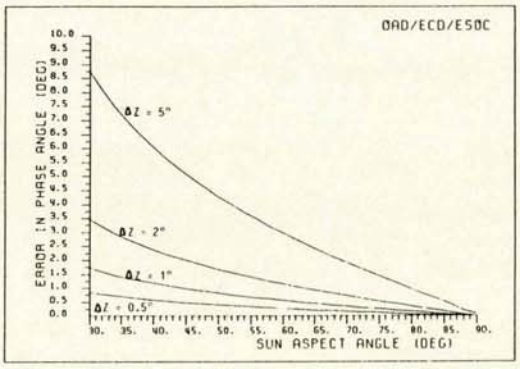

Figure 2.12. Error in phase angle ($\Delta\xi$) as function of sun aspect angle different attitude uncertainties (Δz)

This indicates that the sum $\Delta\xi + \delta_c$ can be accurately determined but that the accuracy σ_{δ_c} is totally dominated by $\sigma_{\Delta\xi}$. Therefore a calibration of the thrust centroid should only be attempted when $\sigma_{\Delta\xi}$ is less than 0.5°. This can only occur for sun aspect angles of 90° + 5°. (See fig. 2.12).

2.3.3 Monitoring attitude/orbit manoeuvres. In section 2.2.2 we pointed out that nearly all attitude and orbit control activities will be directly detected in the Doppler residuals. Since these data are available in the control center in near real time, they can be used to monitor the progress of manoeuvres, as a complement to the spacecraft telemetry data which are essentially limited to the sun aspect angle and the spin period. The changes in radial velocities caused by the manoeuvre will not only indicate satisfactory performances of the thruster but also that EAA follows the predicted trend. For this purpose the cumulative change in radial velocity is compared, every spin period, with the predictions from the manoeuvre preparation program. Unexplainable deviations may help to detect potential problems with the spacecraft or the ground system.

3. ELEMENTS OF THE EARLY ORBIT PHASE OPERATIONS

After separation from the Upper Stage, the spacecraft spin axis lies on a 80° sun cone, roughly opposite to the earth. The nominal EAA is about 150°. By processing 10 to 15 min. of Doppler residuals acquired 4 to 5 hours after separation, the EAA can be accurately determined (see section 2.3). The phase of the signal is used to determine the Earth Phase from the spin axis sun plane (see section 2.2): the intersection between the sun cone and the earth cone provides 2 solutions, the solution which corresponds to the measured Earth Phase Angle is selected.

Thruster Calibration

A complete calibration of the thrusters must be carried out before the first TCM. We have shown how Doppler residuals can be used to calibrate trajectory correction manoeuvres. Attitude manoeuvres are calibrated by observing the changes in sun aspect angle and spin period caused by specially designed manoeuvres. Two points are worth mentioning. First, the calibration of torques as derived from attitude manoeuvres (efficiency factor k, centroid delay δ_c) cannot directly be used as a calibration of forces for delta-v manoeuvres and vice versa. Uncertainties in the moments of inertia and thruster moment arms play a significant role (particularly after deployment of booms) in the calibration of the torques from precession manoeuvres, whereas effects such as plume impingement affect the delta-v calibrations. Therefore, the torques and forces are calibrated in an independent manner. Second, the performance of precession manoeuvres is strongly dependent on the actual spin rate change profile during the manoeuvre: a larger spin rate decreases the performance, first because the angular inertia is increased and, second because the duration of the firing is decreased for a constant pulse width of x degree. Therefore, afer each calibration manoeuvre, the axial component of the torque (affecting the spin rate) is calibrated first, so that the predicted spin rate change (if any) fits the observed change in spin rate. The radial component of the torque is calibrated next.

Taking into account the limitation of the attitude measurement system, two manoeuvres (see figure 3.1) are carried out to calibrate precession manoeuvres for a specific thruster combination and a given duty cycle. One of the manoeuvre precesses the spin axis towards the sun (or away from it) and the change in sun aspect angle, compared to the change predicted (after matching the change in spin rate) will provide the radial torque calibration factor k. Note that for this type of manoeuvre, we can neglect uncertainties in the not yet calibrated thrust centroid delay δ_c. The other manoeuvre precesses the spin axis around the sun cone. A change in sun aspect angle will reflect an error in the torque centroid, thereby providing the data to calculate the centroid delay δ_c. Best results are obtained for sun aspect angles close to 90°. For this second type of manoeuvre, we can neglect uncertainties in k when estimating δ_c. Each calibration (delta-v, precession, spin rate) is validated by implementing the new efficiency factor k and the centroid delay δ_c in the

manoeuvre preparation software and making a detailed pulse by pulse simulation.

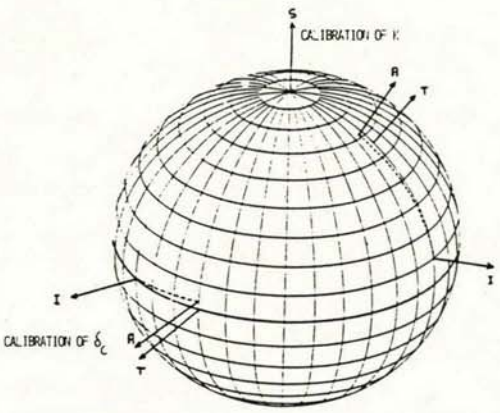

S = SUN DIRECTION
I = INITIAL ATTITUDE
T = TARGET ATTITUDE
SA = OBSERVED SUN ANGLE AFTER MANOEUVRE
A = ACTUAL ATTITUDE

Figure 3.1

Applicable Constraints

For Ulysses, the actual sequence of flight dynamics operations which lead to the execution at day 12 of the first trajectory correction manoeuvre depends on the date of launch. However, the following constraints must always be satisfied:

1) leave 4 days of undisturbed orbit (i.e. no manoeuvre) so that the spacecraft trajectory can be accurately determined

2) acquire the Earth with the HGA, as soon as the sun-probe-earth angle drops below 90° and the spacecraft thermal constraints are satisfied

3) while moving from the injection attitude to the earth pointing attitude, go sufficiently close to sun to estimate the spin axis tilt

4) calibrate to high accuracy one precession thruster to move accurately from the earth pointing attitude to the delta-v pointing attitude and two axial thrusters to provide an accurate axial delta-v

5) calibrate two spin thrusters in pulsed mode so that accurate radial delta v's can be obtained in earth pointing mode.

4. CONCLUSIONS

Joint simulations were carried out for two different launch dates within the May 86 Jupiter window, between the JPL navigation team and the flight dynamics team. Different scenarios resulted for the two launch dates. Both scenarios took into account the techniques proposed above to estimate the earth aspect angle and to calibrate the thrusters from the Doppler residuals. In both cases, the simulations resulted in a successfull mission, although the real proof of the techniques will only be demonstrated in real life, after launch.

Acknowledgement

We wish to thank Mr. H. J. Gordon and Mr. D. Ross of the Jet Propulsion Laboratory, who provided us with real data of Deep Space Probes and produced numerous Doppler data simulations during the ULYSSES Flight Dynamics-Navigation System Tests.

REFERENCES

1. Bright L A and Berman A L 1976, Tracking Operation Analysis Manual I, Jet Propulsion Laboratory.

2. Viskanta V Z and Rose R E, 1972, Conical Scanning System for Pioneer Jupiter Spacecraft, IEEE Transaction on Aerospace and Electronics Systems, Vol. AES-8, No. 2.

3. Wertz J R, Spacecraft Attitude Determination and Control; D. Reidel Publishing Company.

4. AOCS Handbook 1982, ISPM, by Baker K G and Todman D C, British Aerospace Dynamics Group.

5. OAD WP 244 (ESA/ESOC) 1984, ISPM Sun Aspect Angle Determination and Sun Aspect Angle Deadband Setting in the Presence of Spin Axis Tilt, by Goodwin A and Massart A.

6. OAD WP 305 (ESA/ESOC) 1985, Ulysses Real Time Attitude Monitoring Selection of Filter Gains, by A. Massart.

7. OAD WP 276 (ESA/ESOC) 1985, Thruster Modelling for ISPM, by Allcock A and Goodwin A.

8. Farless D L, 1972, Simulation of Tracking Data for Pioneer G, Jet Propulsion Laboratory, IOM 392.6-380.

9. Marini J W, 1970, The Effect of Satellite Spin on Two-Way Doppler Range Rate Measurements, IEEE Transactions on Aerospace Systems, Vol AES-7-No. 2.

10. Wenzel K P and Marsden R G, 1983, The International Solar Polar Mission - Its Scientific Investigation, ESA-SP-1050.